New evaluation method for cold-forge solid phase bonding of dissimilar metals

OKAMOTO Haruki[1,a*], ABE Eiji[1,b], HARADA Hiroshi[1,c] and YUKAWA Nobuki[1,d]

[1]Department of Material Science and Engineering, Nagoya University, Furo-cho, Chikusa-ku, Nagoya, Aichi 464-8601, Japan

[a]okamoto@mp.material.nagoya-u.ac.jp, [b]abe.eiji@material.nagoya-u.ac.jp, [c]harada.hiroshi@material.nagoya-u.ac.jp, [d]yukawa@nagoya-u.jp

Abstract. Solid phase bonding is an effective method for joining dissimilar metals. Solid phase bonding is the bonding method without fusing metal matrix. Using this method, clad metal which is joined with sheet metals is in practice. However, the parameters to achieve stable cold-forge solid phase bonding in bulk are not well known. To investigate the parameters that affect the solid phase bonding state, a new test method to evaluate the strength of the bonding interface obtained by cold forging was developed. Using this method, test pieces bonded with S10C/A1070 and SUS304/A1070 were made in fluctuating interface bonding parameters (the surface area expansion ratio, the surface pressure). Although tensile test results showed large variation in joining strength at low value of bonding parameters, bonding was strong enough to exceed the A1070 base metal strength at the region of high value of bonding parameters. As it was found that the bonding parameters were able to measure the effect on joining strength in this experiment, it is considered that bonding parameters for solid phase bonding can be evaluated by the newly developed test method.

Introduction

To reduce the weight of automobiles, demand for technology to join dissimilar metals increases [1]. For instance, high-strength, high-rigidity steel materials and low-density aluminum alloy materials are tried to join. However, it is difficult to bond dissimilar metals (particularly Fe/Al) strongly by fusion welding because of the occurrence of thick intermetallic compounds (IMCs), such as Al_3Fe, Al_5Fe_2, and Al_2Fe [2]. These IMCs reduce the joining strength of the Fe/Al interface when the IMC thickness is in the range of 0.5–2μm or over [3, 4]. Solid phase bonding is an effective method for bonding dissimilar metals as thick IMCs are difficult to form. Bonding methods that utilize plastic deformation [4, 5] are classified into two types. Mechanical bonding such as lock seam processing [6] and mechanical clinching, a type of caulking joining method [1, 7]. Metallurgical methods that utilize metallic bonding through exposure and close contact with nascent surfaces caused by plastic deformation [8]. For instance, FSW [9], explosive welding [10], diffusion bonding [11, 12] and cold-forge solid-phase bonding. In this study, the latter, especially cold-forge solid-phase bonding was focused on. To bond steel and aluminum, both metals are deformed at the same time by forging, and the contact surface area of each metal is expanded. Surface area expansion breaks the brittle [13, 14] oxide layer on the metallic surface and exposes nascent surface. Pressure is applied to the nascent surface, and bonding is made by bringing it into contact (Fig. 1 [8]). Since this bonding method does not require external heat input, no or only a small amount of brittle IMC layer at the bonding interface is generated [12, 15]. Since no heat input is required, it is environmentally friendly and inexpensive. Clad metal bonded by the same mechanism is in practice. However, the parameters to achieve stable cold-forge solid phase bonding in bulk are not well known. Currently, the factors that are considered to affect bonding (bonding parameters) are the surface area expansion ratio of the base metal [16, 17], the surface

pressure on the interface [16], and the relative slip amount [16, 18]. The goal is to quantitatively evaluate the influence of these bonding parameters on forge solid phase bonding. Previous research has shown that this method can provide a certain degree of bonding strength and relationship between bonding parameters and joining strength can be suggested to some extent too. However, it was not possible to make test pieces with a wide range of joining parameters. In addition, it can not measure joining strength accurately because mechanical clinching was found on the interface and the bonding interface was not plane. Due to the inadequacy of this methods, it was difficult to evaluate bondability with a wide range of bonding parameters and it was not possible to evaluate the strength of the solid phase bonding itself. In this study, to improve the problems, a new evaluate method to measure joining strength accurately was developed. With this new test method, it is possible to make test pieces bonded with a wide range of bonding parameters compared with previous one. Moreover, they are applied tensile load perpendicular to the plane bonding interface.
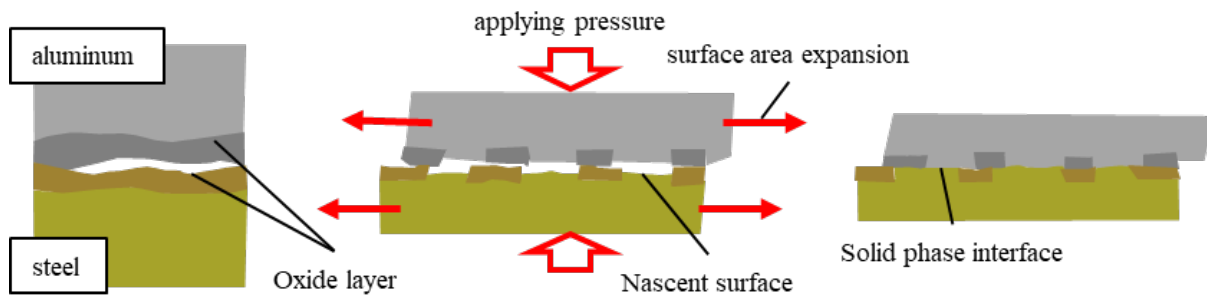

Fig.1. Image of Cold-Forged Solid Phase Bonding [8].

New Evaluation / Experimental Condition

A newly developed method to evaluate solid phase bonding is shown in Fig. 2. First, the center of the S10C or the SUS304 cylinders was hollowed out, and the A1070 cylinder was inserted into it. They were plugged into a rigid restraint die with a hole in the center and a height of 10mm. They were forged restraining the lower part with a concentric grooved restraining upper die. Solid phase bonding is expected to be achieved at the red line shown in the Fig. 2. With this forging method, it is possible to forge aluminum while applying strong back pressure, so to expand the surface area of steel and aluminum at the same time, which have significantly different yield stresses. As the lower part of the cylinder was restrained by a die, a sufficient grip section was secured on the aluminum part in performing the tensile test. Using this method, the affection of bonding parameters could be investigated. Tensile test pieces can be made with large wide bonding parameters by changing the thickness of steel (t_{Fe}), the diameter of aluminum (φd_{Al}), and reduction. In this study, to evaluate the joining strength, the tensile test was performed on test pieces prepared material combination of S10C/A1070 and SUS304/A1070. As shown in Fig. 3, tensile test pieces were cut from the center of forged metal by wire electric discharge machining (WEDM). To remove the heat effect area caused by WEDM, 0.25 mm of the outer diameter of the test piece was removed by turning [19]. Notches were added to the steel to hook the jig. Using this processed test piece, a tensile test was performed.
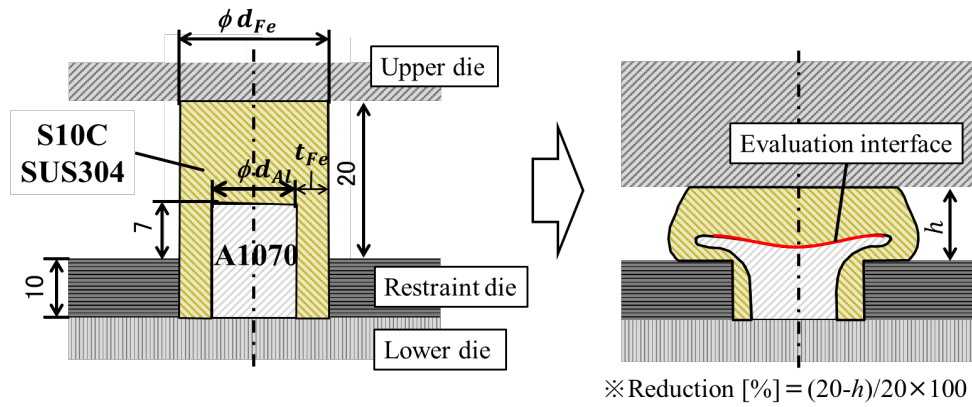
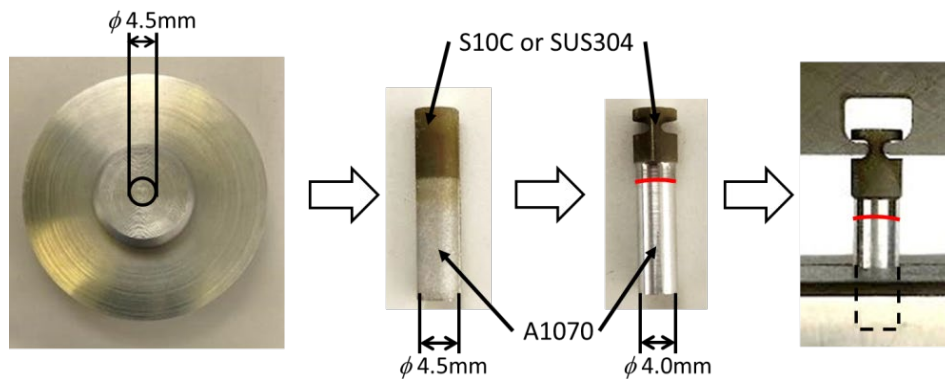Fig. 2. Experimental overview for new evaluation method.

Fig. 3. Tensile test to measure joining strength.

In hollowing out the center of steel (S10C, SUS304), the end mill was thrust to the bottom of the steel. The profile curve was measured by using stylus surface roughness measurement (probe radius is 0.2 μm, tip angle is 60°, measurement speed is 0.25 mm/sec) to know the effect of roughness within a range of ±2mm in the radial direction from the center of S10C, SUS304 and A1070. The profile curve of S10C and SUS304 were shown in Fig. 4. In this result, the center of steel is about 70 µm higher than the location of 2 mm away from the center because the end mill can not cut the central area. The arithmetic average roughness (S10C, SUS304, A1070) was calculated. Results are shown in Table 1.
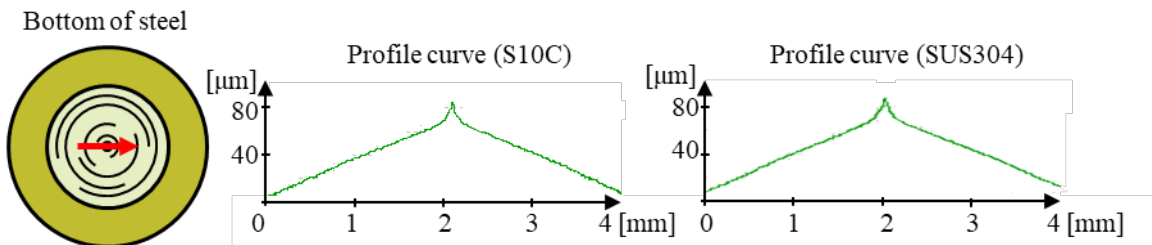

Fig. 4. profile curve of the evaluation interface of Fe side before bonding.

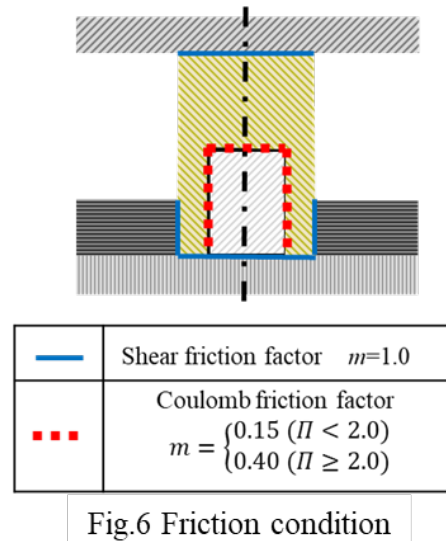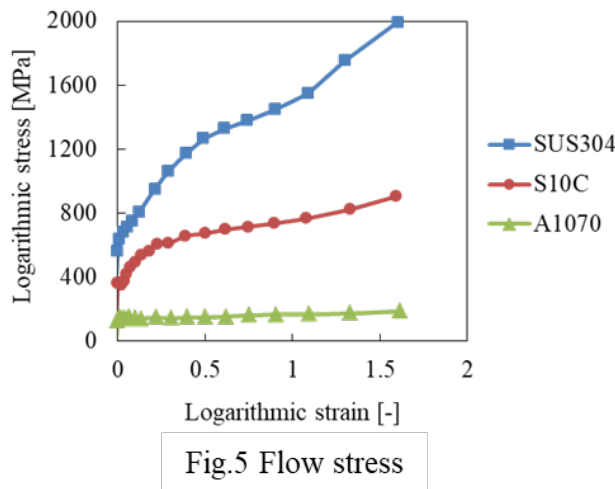Table 1. Arithmetic average roughness (Ra) of S10C, SUS304, A1070.

Material	Ra [μm]
S10C	0.153
SUS304	0.096
A1070	0.112

New Evaluation / FEM Condition

To know the interface condition, bonding parameters (the surface area expansion ratio, the surface pressure, and the relative slip amount) were calculated using FEM. Finite element analysis software, DEFORM-2D was used. Conditions and assumptions for analysis were defined as shown in Table 2. FEM model was Axisymmetric, S10C, SUS304 and A1070 were regarded as elasto-plastic, die and restraint die were regarded as rigid.The compression speed was defined to match the one of the actual press machine. Flow stress for each material shown in Fig. 5 was determined by compression test with repeated lubrication. The friction conditions shown in Fig. 6 were determined so that the cross section diagram of the contact interface matched with experimental results. The coulomb friction factor was 0.15 when the surface area expansion ratio ($= \Pi$) was less than 2.0, and 0.4 when Π exceeded 2.0 on the interface of steel/aluminum. As upper die is a concentric grooved restraining and lower part of cylinder was completely restrained, other contact conditions were regarded as sticking friction. Thermal effect was neglected.

Table 2. FEM conditions.

Model	Axisymmetric
Deformation condition	S10C・SUS304・A1070：Elasto-plastic Die・Restraint Die：Rigid
Materials	S10C-A1070, SUS304-A1070
Young's modulus	S10C：206[GPa] SUS304：197 [GPa] A1070：69[GPa]
Poisson's ratio	S10C：0.30 SUS304：0.30 A1070：0.33
Compression speed	0.607 [mm/sec]

Fig.5 Flow stress

	Shear friction factor $m=1.0$		
	Coulomb friction factor $m = \begin{cases} 0.15 \ (\Pi < 2.0) \\ 0.40 \ (\Pi \geq 2.0) \end{cases}$		

Fig.6 Friction condition

Result of FEM

Bonding parameters (the surface area expansion ratio, the surface pressure, and relative slip amount) were varied by changing the reduction, the diameter of aluminium (φd_{Al}), and the thickness of steel (t_{Fe}). Fig. 7 shows the calculated bonding parameter distribution along the S10C/A1070 and SUS304/A1070 interface obtained from the results of FEM under the conditions of t_{Fe}=3mm, φd_{Al}=10mm. The relationship between reduction and the surface pressure was shown in Fig. 7(a), (b). The black dashed line in Fig. 7 indicates the location where the test piece was taken. As reduction increased, the surface pressure increased. In SUS304/A1070, nearly twice the surface pressure compared with S10C/A1070 was obtained. The relationship between reduction and the surface area expansion ratio was shown in Fig. 7(c), (d). The surface area expansion ratio of SUS304/A1070 was small compared to S10C/A1070. In both metal combinations, the surface pressure and the surface area expansion ratio were almost constant in the location where the test piece was taken. The relationship between reduction and the relative slip amount was shown in Fig. 7(e), (f). Although the relative slip amount increased as the reduction increased, it was considered to be very small in the radial location of 0-2 mm compared to the relative slip amount in previous research [16, 18]. The cold-forge solid phase bonding of high tensile strength steel and aluminium alloy sheets by miwada [16], it is shown that approximately 0.1-0.4 mm of the relative slip amount was observed on the bonding interface. In this study, approximately 0-0.002 mm of the relative slip amount was observed. Therefore, only the surface area expansion ratio and the surface pressure were focused on.
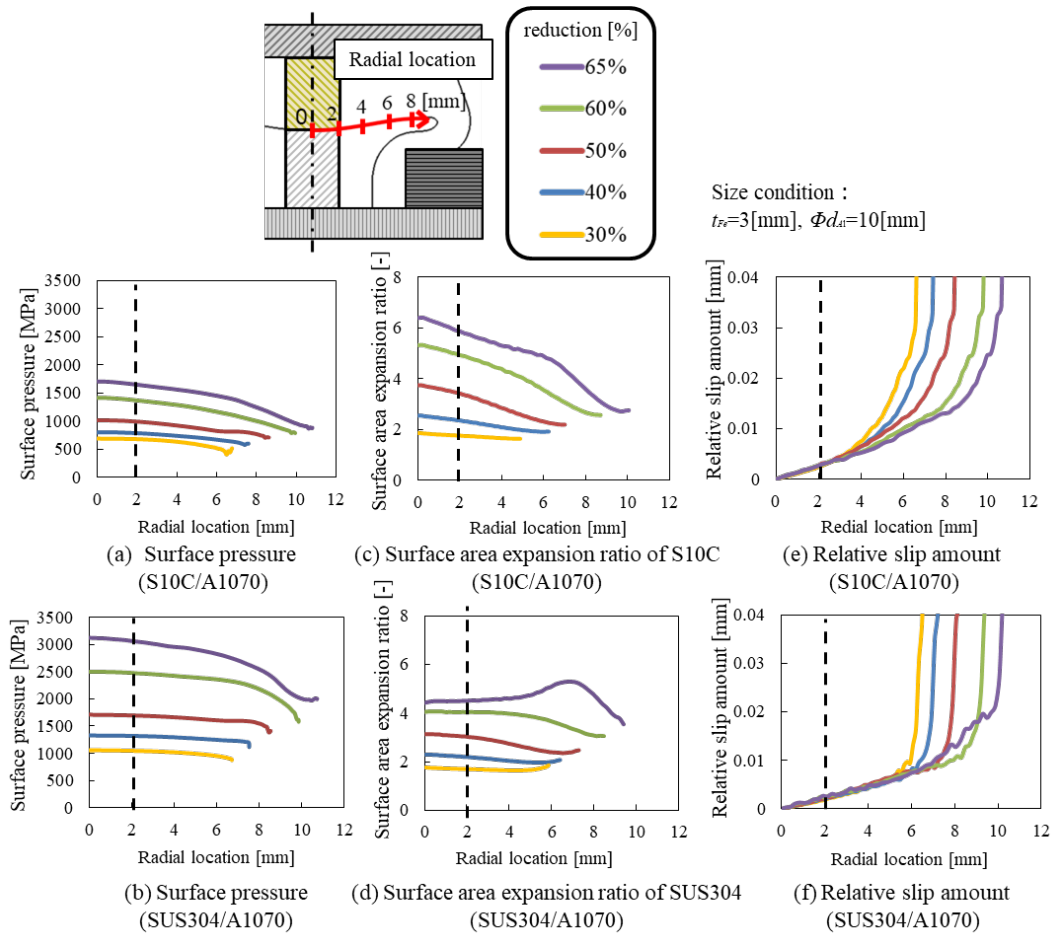
Fig. 7. Distribution of bonding parameters.

The effect of t_{Fe} and φd_{Al} changes on bonding parameters was investigated under the condition of a reduction of 60%. The relationship between t_{Fe}, φd_{Al}, and the surface area expansion ratio, the surface pressure were plotted shown in Fig. 8. The surface area expansion ratio and the surface pressure were average values in the radial location of 0-2 mm. Fig. 8(a) showed the distribution for S10C/A1070, and Fig. 8(b) showed the distribution for SUS304/A1070. The correspondence of shape on the graph was shown in Table 3. In both metal combinations, as t_{Fe} was increased, the surface pressure increased, and the surface area expansion ratio decreased. A similar tendency was observed when φd_{Al} was increased. It was also found that SUS304/A1070 is difficult to vary the surface area expansion ratio over a wide range compared to S10C/A1070. From the results of Fig. 8, it was suggested that it was possible to adjust the bonding parameters on the interface to some extent by changing the size of S10C, SUS304 and, A1070. As an example of the way to use, in S10C/A1070, by comparing a test piece made of t_{Fe}=4 mm, φd_{Al}=8 mm with t_{Fe}=3 mm, φd_{Al}=10 mm under the condition of a reduction of 60%, only the effect of surface area expansion ratio on solid phase bonding could be investigated while keeping the surface pressure at the same level. It is considered to be valid as a test method to investigate bonding conditions.
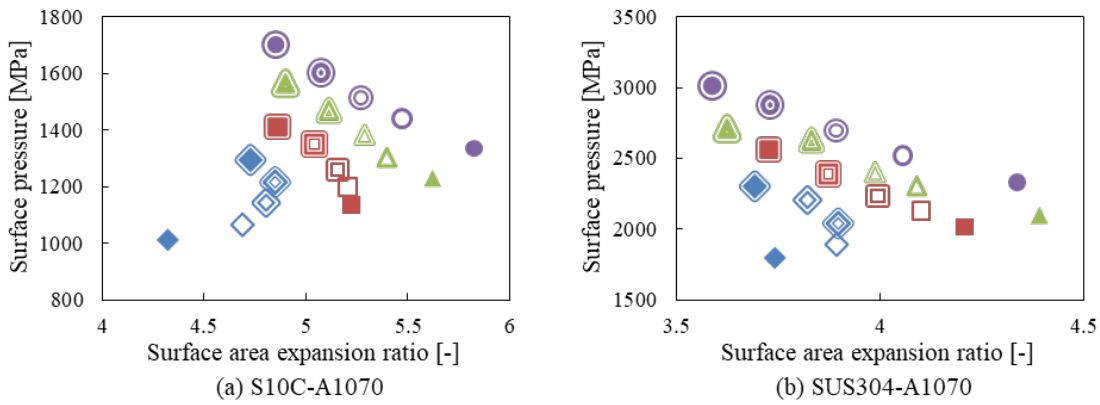
(a) S10C-A1070   (b) SUS304-A1070

Fig. 8. Relationship between surface area expansion ratio and surface pressure.

Table 3. Correspondence of shapes on the graph.

Tensile Test Result

Tensile test pieces bonded with S10C/A1070 and SUS304/A1070 were made under the conditions of t_{Fe}=3mm, φd_{Al}=10mm. Fig. 9(a), (b) shows the results of tensile tests by the relationship between reduction and joining strength. The result of the metal combination of S10C/A1070 is shown in Fig. 9(a) and SUS304/A1070 is shown in Fig. 9(b). Fig. 10(a), (b) shows the relationship between the surface area expansion ratio (average value in 0-2mm radial distance) and joining strength. The result of the metal combination of S10C/A1070 is shown in Fig. 10(a) and SUS304/A1070 is shown in Fig. 10(b). And Fig. 11(a), (b) shows the relationship between the surface pressure (average value in 0-2 mm radial distance) and joining strength. The result of the metal combination of S10C/A1070 is shown in Fig. 11(a) and SUS304/A1070 is shown in Fig. 11(b). In Figs. 9, 10, 11, red plots show the results of tensile test pieces that could be measured joining strength, blue cross marks show them broken in cutting by WEDM. The surface area expansion ratio and the surface pressure are the average values on the interface of test pieces. In both metal combinations, as reduction increased, as the values of bonding parameters were increased, joining strength was increased. Some of the test pieces with low reduction were scarcely bonded, they were broken by cutting by WEDM due to residual stress [20]. On the other hand, test pieces forged with high reduction showed their joining strength about 130 MPa. To investigate the effect of work hardening in forging, micro Vickers hardness test (load was 0.245, time was 15s) was held as shown in Fig. 12. In range of 1.5mm×4.0 mm, about 100 points, Vickers hardness was measured and drew the distribution in three condition (S10C-A1070 reduction 50%, S10C-A1070 reduction 62.5%, SUS304-A1070 reduction 50%). From the test results in Fig. 13, it was recognized that work hardening was clearly observed in approximately 0-1 mm downward from the interface considering A1070 base metal Vickers hardness was 40HV0.025 in all experimental

conditions. It is thought that the joining strength which was the same level as the tensile strength of A1070 base metal was obtained under the condition of high reduction.
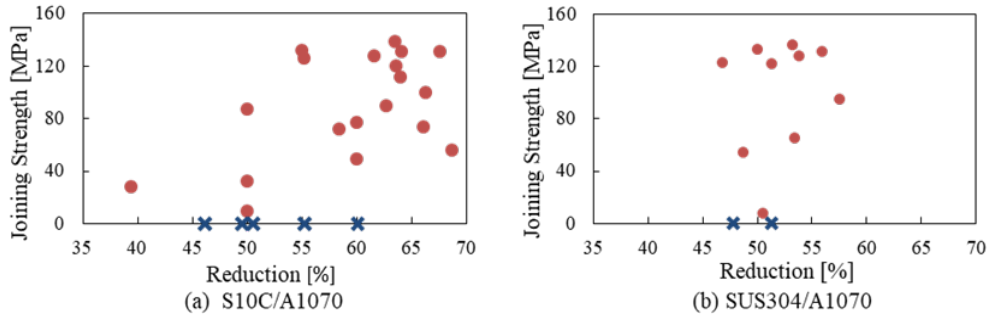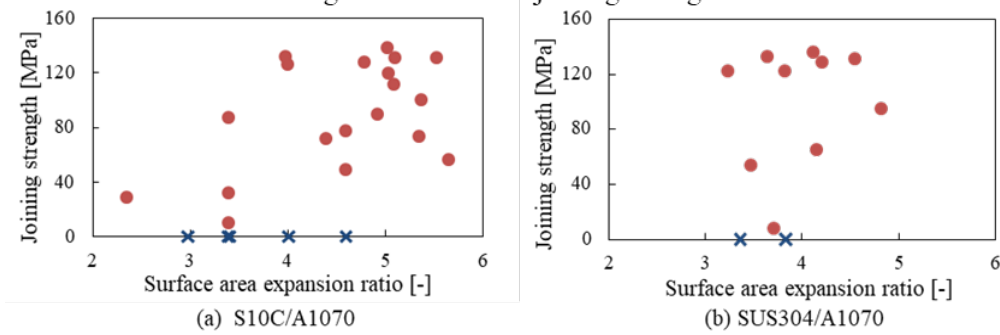

(a) S10C/A1070   (b) SUS304/A1070
Fig.9 Reduction vs joining strength

(a) S10C/A1070   (b) SUS304/A1070
Fig.10 Surface area expansion ratio vs joining strength
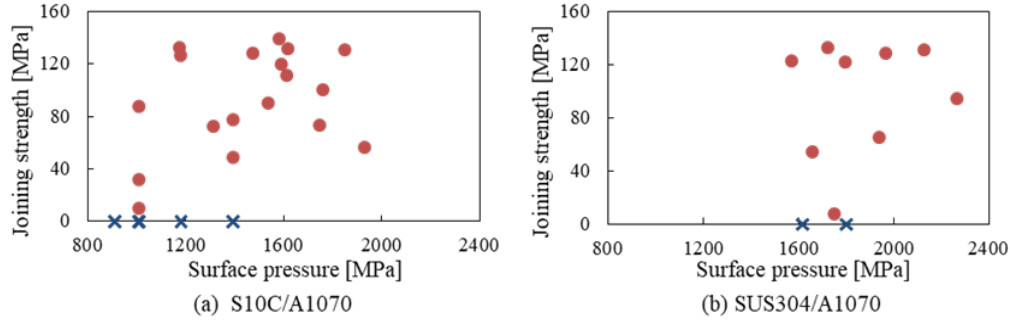

(a) S10C/A1070   (b) SUS304/A1070
Fig.11 Surface pressure vs joining strength

● : Test piece that tensile strength could be measured
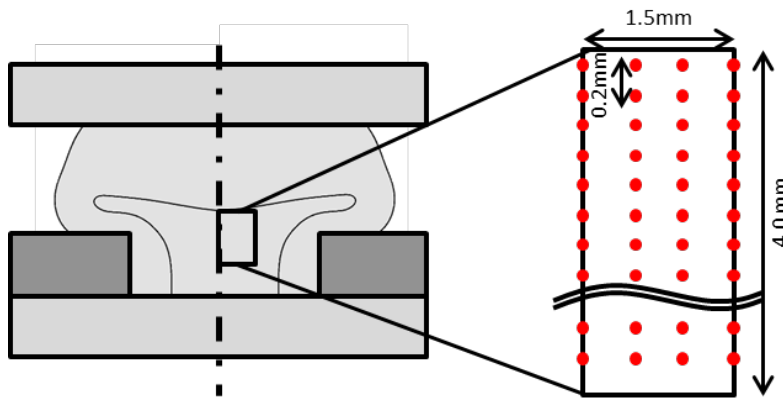✕ : Test piece broken by cutting with WEDM

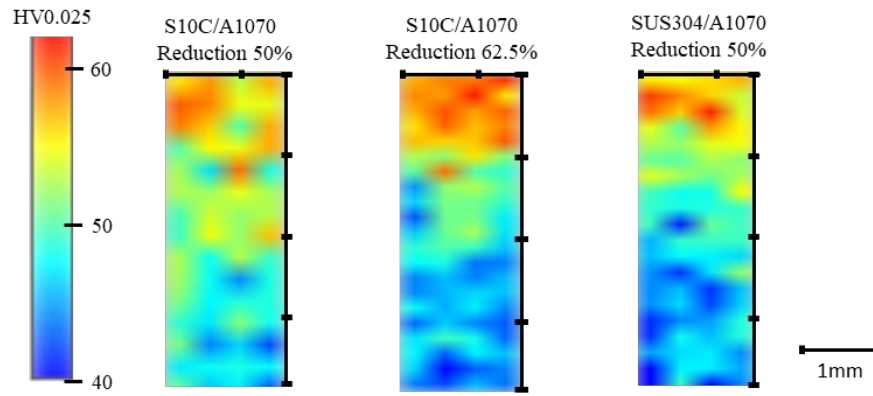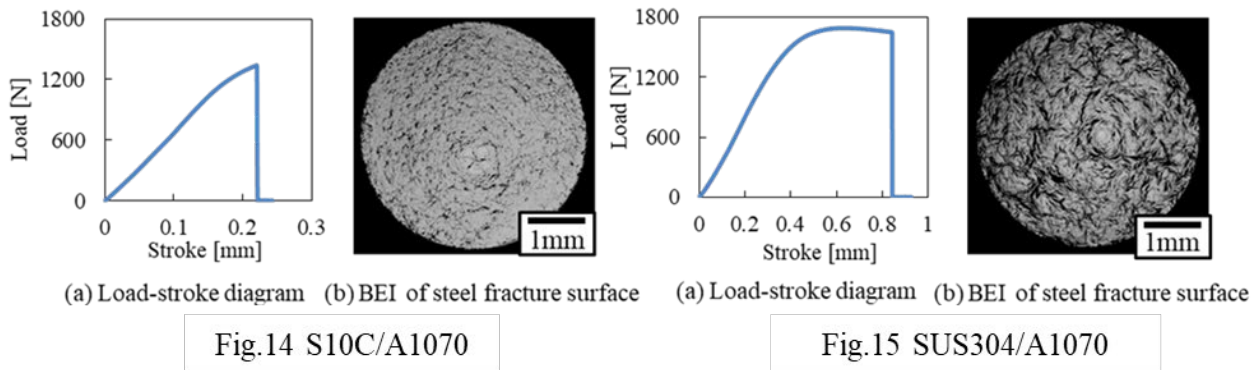Fig. 12. Vickers hardness test measurement position.

Fig. 13. Vickers hardness distribution.

Fig. 14(a), Fig. 15(a) show load-stroke diagram of the tensile test results of S10C/A1070 and SUS304/A1070 respectively which showed highest joining strength, and Fig. 14(b), Fig. 15(b) show backscattered electron image (BEI) of steel side fracture surface after the tensile test in the combination of S10C/A1070 and SUS304/A1070 respectively. S10C/A1070 was a macroscopically brittle failure, while SUS304/A1070 showed elongation from Fig. 14(a) and Fig. 15(a). The black part is the adhesion of the aluminum in BEI. The amount of adhesive rate of aluminum on the steel side fracture surface was obtained from these BEIs. SUS304/A1070 gained high adhesive rate compared to S10C/A1070 from Fig. 14(a) and Fig. 15(b). One of the reasons for the large variation of tensile test results is thought to be the low adhesive rate. When there are large defects in size or in number on the interface, it is easier to be in brittle fracture. Fig. 16(a), (b) showed relationship between adhesive rate and joining strength in the combination of S10C/A1070 and SUS304/A1070, respectively. It was shown that the higher the adhesive rate it was, the less variation there was and the more stable joining strength was showed. It seems that it shows the importance of increasing the adhesion rate in order to achieve stable and strong bonding.
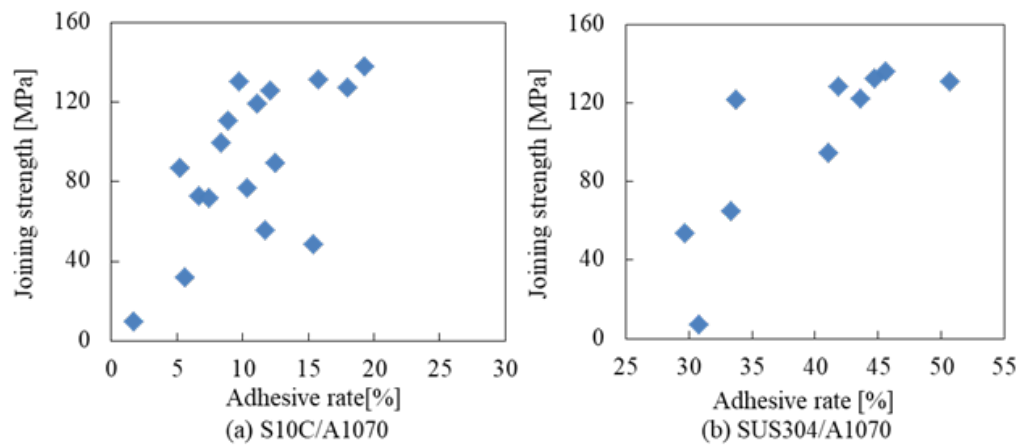

(a) Load-stroke diagram   (b) BEI of steel fracture surface

Fig.14 S10C/A1070

(a) Load-stroke diagram   (b) BEI of steel fracture surface

Fig.15 SUS304/A1070

Fig. 16. Relationship between adhesive rate and joining strength.

Summary

The parameters required to achieve forge solid phase bonding was investigated by doing the experiment and FEM.

・The test method that can accurately measure the joining strength was developed.

・In this bonding method, Fe/Al could be bonded under a wide range of the surface area expansion rate and surface pressure. The constant distribution of the surface pressure and the surface area expansion ratio was obtained in the region of the interface of tensile test pieces.

・Using a newly developed test method, joining strength was measured in combinations of S10C/A1070 and SUS304/A1070 by changing reduction. In both combinations, as reduction increased, joining strength was increased.

・Although variation was observed, the effect of reduction was shown in the results of the tensile test. Fe/Al could be bonded strongly by cold-forge solid phase bonding, some test pieces showed joining strength was about 130MPa.

・Some test pieces in SUS304/A1070 were broken in ductility. Observing the BEI of the steel side fracture surface after the tensile test, nearly twice the adhesive rate of SUS304/A1070 was obtained compared with S10C/A1070. It is thought difference in adhesion rate affects fracture form.

References

[1] Fujimoto yuichiro, Urushiyama Yuta, Automotive multi-material strategy (2017) 115-127, in Japanese.

[2] ASM HANDBOOK vol.3 (2016) 133.

[3] H. Yamagisi, High-productivity and high-strength Fe/Al dissimilar metal joining by spot forge welding, Mater. Lett. 278 (2020) 128412. https://doi.org/10.1016/j.matlet.2020.128412

[4] K. Martinsen, Joining of dissimilar materials, CIRP Annals-Manuf. Tech. 64 (2015) 679-699. https://doi.org/10.1016/j.cirp.2015.05.006

[5] R.F. Tylecote, The Solid Phase Welding of Metals, Edward Arnold Ltd., (1968) 226-318.

[6] Y. Fang, W. Gai, H. Yang, B. Lu, Modelling and lock-seam effects on compressive behaviour of concrete-filled helical corrugated steel tubes, Structure 58 (2023) 105321. https://doi.org/10.1016/j.istruc.2023.105321

[7] Y. Abe, K. Mori, T. Kato, Joining of high strength steel and aluminium alloy sheets by mechanical clinching with dies for control of metal flow, J. Mater. Process. Tech. 212 (2012) 884-889. https://doi.org/10.1016/j.jmatprotec.2011.11.015

[8]   N. Bay, Trans. ASME, J. Eng. Ind. 101 (1979) 121-127.

[9]   X. Liu, Analysis of process parameters effects on friction stir welding of dissimilar aluminum alloy to advanced high strength steel, Metal. Des. 59 (2014) 50-62. https://doi.org/10.1016/j.matdes.2014.02.003

[10] S.H. Carpenter, R.H. Wittman, Annual Review of Mater. Sci. (1975) 177-199.

[11] M.G. Nicholas, R.M. Crispin, Diffusion bonding stainless steel to alumina using aluminium interlayers, J. Mater. Sci. 17 (1982) 3347-3360. https://doi.org/10.1007/BF01203505

[12] G. Chen, X. Chang, G. Liu, Q. Chen, F. Han, S. Zhang, Z. Zhao, Formation of metallurgical bonding interface in aluminum-steel bimetal parts by thixotropic-core compound forging, J. Mater. Process. Tech. 283 (2020) 116710. https://doi.org/10.1016/j.jmatprotec.2020.116710

[13] D. Chicot, Mechanical properties of magnetite (Fe_3O_4), hematite (α-Fe_2O_3) and goethite (α-$FeO \cdot OH$) by instrumented indentation and molecular dynamics analysis, Mater. Chem. Phys. 129 (2011) 862-870. https://doi.org/10.1016/j.matchemphys.2011.05.056

[14] M.K. Tripp, The mechanical properties of atomic layer deposited alumina for use in micro- and nano-electromechanical systems, Sensors and Actuators A: Physical 130-131 (2006) 419-429. https://doi.org/10.1016/j.sna.2006.01.029

[15] H. Yamagishi, Spot Forge-Welding for Rapid Dissimilar Joining of Fe to Al to Produce an Intermetallic Compound-Free Interface, Mater. Trans. 62 (2021) 1576-1582. https://doi.org/10.2320/matertrans.MT-M2021080

[16] Y. Miwada, T. Ishiguro, E. Abe, N. Yukawa, T. Ishikawa, T. Suganuma, Cold Forge Spot-bonding of High Tensile Strength Steel and Aluminum Alloy Sheets, Procedia Eng. 81 (2014) 2006-2011. https://doi.org/10.1016/j.proeng.2014.10.272

[17] P. Groche, S. Wohletz, A. Erb, A. Altin, Effect of the primary heat treatment on the bond formation in cold welding of aluminum and steel by cold forging, J. Mater. Process. Tech. 214 (2014) 2040-2048. https://doi.org/10.1016/j.jmatprotec.2013.12.021

[18] R. Matsumoto, Improvement in bonding strength by applying circumferential sliding in cold copper/aluminum forge-bonding, J. Mater. Process. Tech. 307 (2022) 117685. https://doi.org/10.1016/j.jmatprotec.2022.117685

[19] L. Straka, I. Corny, J. Borzikova, Strojarstvo 51 (2009) 633-640.

[20] S. Ossenkemper, C. Dahnke, Analytical and experimental bond strength investigation of cold forged composite shafts, J. Mater. Process. Tech. 264 (2019) 190-199. https://doi.org/10.1016/j.jmatprotec.2018.09.008